

# Fluorescence depolarization in a scattering medium: Effect of size parameter of a scatterer

N. Ghosh, S. K. Majumder, and P. K. Gupta\*

Biomedical Applications Section, Centre for Advanced Technology, Indore 452013, India

(Received 18 June 2001; published 23 January 2002)

For a monodisperse scattering medium, we investigate the dependence on scatterer size parameter for the change in anisotropy of fluorescence due to single scattering at excitation or emission wavelength. The value for the ratio of the anisotropy of fluorescence after one scattering at excitation or emission wavelength to the initial value was observed to increase with increasing value of scatterer size parameter. The effect of multiple scattering on anisotropy of fluorescence from fluorophores embedded in a scattering medium was incorporated using a photon migration model. The model was validated by experiments carried out on samples with known concentration of polystyrene microspheres as scatterers and riboflavins or reduced form of nicotinamide adenine dinucleotide as fluorophores.

DOI: 10.1103/PhysRevE.65.026608

PACS number(s): 42.25.Ja, 42.25.Dd

## I. INTRODUCTION

It is well known that even when excited by polarized light, the emission from fluorophores gets depolarized due to several processes such as the random orientation and rotational diffusion of fluorophores and the radiationless energy transfer among fluorophores [1]. In a scattering medium, depolarization can also occur due to multiple scattering of both the excitation and emission light. In the limit of Rayleigh scattering it has been shown earlier [2] that after each scattering event at excitation or emission wavelength fluorescence anisotropy reduces to 0.7 times its initial value. However, to the best of our knowledge, the dependence of the reduction in anisotropy of fluorescence after single scattering at excitation or emission wavelength on size of the scatterer has not been addressed. There do exist some studies on the effect of concentration and size of the scatterer on the degree of depolarization of elastically scattered light [3–8]. These studies reveal that with an increase in the value of size parameter of scatterer ( $x = 2\pi aN/\lambda$ , where  $a$  is the radius of scatterer,  $\lambda$  the wavelength and  $N$  the ratio of the refractive index of the scatterer to the surrounding medium), the characteristic length of depolarization of linearly polarized light increases significantly. It therefore follows that the value of the reduction in fluorescence anisotropy after single scattering event should also depend on the size parameter of scatterer.

We report here a theoretical treatment for the dependence of the change in anisotropy of fluorescence after single scattering at excitation or emission wavelength on the scatterer size parameter. For a monodisperse scattering medium, the value of the parameter  $r_0$ , defined as the ratio of fluorescence anisotropy after single scattering to the initial anisotropy, was observed to vary from 0.65 to 0.85 for a variation in scatterer size parameter of  $0 < x < 20$ .

For evaluating anisotropy of fluorescence from a scattering medium the effect of multiple scattering was incorporated using a photon migration model. The results of the experiments carried out on samples with known concentra-

tion of polystyrene microspheres as scatterers and NADH (nicotinamide adenine dinucleotide) or riboflavins as fluorophores are in reasonable agreement with the theory.

## II. THEORY

### A. Depolarization produced by single scattering

We first develop a theoretical treatment for depolarization of fluorescence by single scattering of the excitation light for typical  $L$ -format measurement geometry shown in Fig. 1.

Excitation light polarized along  $X$  direction and propagating along  $Z$  direction is scattered by a spherical scatterer situated at  $O$ . The scattered light excites fluorophore located at  $P(r, \theta, \varphi)$  [where  $\theta$  is the scattering angle and  $\varphi$  is the azimuth angle]. A laboratory polarizer kept along  $X$ - $Z$  plane of a  $L$ -format detection geometry detects fluorescence intensities  $I_X$  and  $I_Z$ , respectively, as polarization parallel ( $I_{\parallel}$ ) and perpendicular ( $I_{\perp}$ ) to incident polarization of the excitation light. In terms of these measurements the observed polarization ( $P'$ ) and anisotropy ( $A'$ ) of fluorescence is given by

$$P' = (I_{\parallel} - I_{\perp}) / (I_{\parallel} + I_{\perp}) \quad (1)$$

and

$$A' = (I_{\parallel} - I_{\perp}) / (I_{\parallel} + 2I_{\perp}). \quad (2)$$

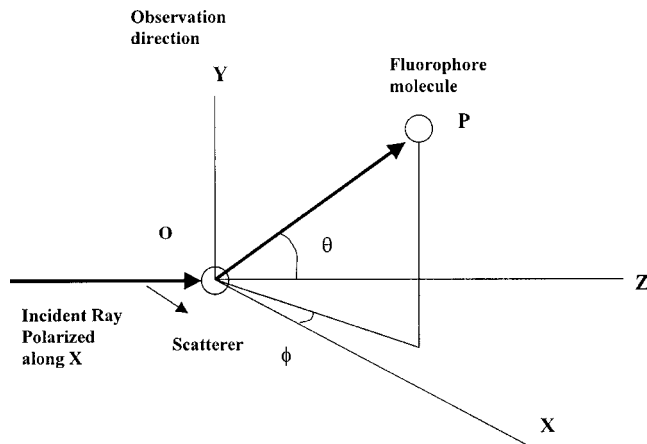


FIG. 1. Basic geometry for fluorescence anisotropy measurement.

\*Email address: pkgupta@cat.ernet.in

For the sake of simplicity, let us ignore intrinsic causes of depolarization and assume that fluorophore emits light with same polarization as that of the excitation light. In this approximation the observed values for  $P'$  and  $A'$  can be determined by working out the components of the scattered intensity reaching the fluorophore along  $X, Y$ , and  $Z$  direction. Since the emitted fluorescence in such case will have same polarization as that of the scattered light, the observed anisotropy of fluorescence viewed through the laboratory polarizer kept along  $X$ - $Z$  plane will thus be

$$A' = (I_X - I_Z) / (I_X + 2I_Z). \quad (3)$$

For spherical scatterer, the intensity components  $I_X, I_Y$ , and  $I_Z$  can be worked out using single scattering calculations based on Mie theory [9]. For this the incident electric field vector ( $E_{0X}$ ) at point  $O$  was resolved into components  $E_{OX'}$  and  $E_{OY'}$  parallel and perpendicular to the scattering plane (plane defined by the wave vector of incident and scattered light), respectively,

$$E_{OX'} = E_{0X} \cos \phi$$

and

$$E_{OY'} = -E_{0X} \sin \phi, \quad (4)$$

where  $E_{0X}$  is the incident electric field vector and  $Z'$  is the direction of the scattered ray.

The amplitudes of the electric fields polarized parallel and perpendicular to scattering plane at  $P(r, \theta, \phi)$  can be written as

$$E_{X'} = S_2(\theta) \{ \exp(-ikr + ikz) / ikr \} E_{OX'}$$

and

$$E_{Y'} = S_1(\theta) \{ \exp(-ikr + ikz) / ikr \} E_{OY'}, \quad (5)$$

where  $S_2(\theta)$  and  $S_1(\theta)$  are the scattering amplitudes and can be computed using Mie theory for a spherical scatterer. The amplitudes of the scattered fields in the laboratory coordinate ( $E_X, E_Y$ , and  $E_Z$ ) can be obtained in terms of  $E_{X'}$  and  $E_{Y'}$ . This can be conveniently done by two successive Euler rotation of coordinate system. The coordinates ( $X', Y', Z'$ ) after scattering can be related to ( $X, Y, Z$ ) of the laboratory coordinate by first rotating ( $X, Y$ ) anticlockwise at an angle  $\phi$  about  $Z$  to reach a new coordinate system ( $X'', Y', Z$ ) and then once again rotating ( $X'', Z$ ) anticlockwise at an angle  $\theta$  about  $Y'$ . The amplitudes of the scattered electric field vectors ( $E_X, E_Y$ , and  $E_Z$ ) can thus be obtained as

$$E_X = \cos(\theta) \cos(\phi) E_{X'} - \sin(\theta) \cos(\phi) E_{Y'} + \sin(\theta) \sin(\phi) E_{Z'},$$

$$E_Y = \cos(\theta) \sin(\phi) E_{X'} + \cos(\theta) \sin(\phi) E_{Y'} + \sin(\theta) \cos(\phi) E_{Z'},$$

$$E_Z = -\sin(\theta) E_{X'} + \cos(\theta) E_{Z'}. \quad (6)$$

Here,  $E_{Z'} = 0$ , since there will be no component of electric field along the direction of scattered ray. The corresponding intensity components are

$$I_X = E_X E_X^* = (1/4\pi) [ P_2(\theta) \cos^2(\theta) \cos^4(\phi) + P_1(\theta) \sin^4(\phi) + 2\{P_2(\theta)P_1(\theta)\}^{1/2} \cos(\theta) \sin^2(\phi) \cos^2(\phi) ] \times (\pi a^2 Q_s / k^2 r^2) I_{0X},$$

$$I_Y = E_Y E_Y^* = (1/4\pi) [ P_2(\theta) \cos^2(\theta) \sin^2(\phi) \cos^2(\phi) + P_1(\theta) \sin^2(\phi) \cos^2(\phi) - 2\{P_2(\theta)P_1(\theta)\}^{1/2} \cos(\theta) \sin^2(\phi) \cos^2(\phi) ] \times (\pi a^2 Q_s / k^2 r^2) I_{0X},$$

$$I_Z = E_Z E_Z^* = (1/4\pi) [ P_2(\theta) \sin^2(\theta) \cos^2(\phi) ] \times (\pi a^2 Q_s / k^2 r^2) I_{0X}, \quad (7)$$

where  $P_2(\theta)$  and  $P_1(\theta)$  are the scattering phase functions of scattered light polarized parallel and perpendicular to the scattering plane for a spherical scatterer of radius  $a$  and of scattering efficiency  $Q_s$ ,

$$|S_1(\theta)|^2 = [P_1(\theta) / 4\pi] (\pi a^2 Q_s)$$

and

$$|S_2(\theta)|^2 = [P_2(\theta) / 4\pi] (\pi a^2 Q_s), \quad (8)$$

$I_{0X}$  is the incident intensity.

The total scattered intensities can be obtained by summing up the contributions for  $\theta$  varying between 0 to  $\pi$ , and  $\phi$  varying between 0 to  $2\pi$  as

$$I_X^{\text{tot}} \approx \int \int I_X \sin(\theta) d\theta d\phi,$$

$$I_Y^{\text{tot}} \approx \int \int I_Y \sin(\theta) d\theta d\phi,$$

and

$$I_Z^{\text{tot}} \approx \int \int I_Z \sin(\theta) d\theta d\phi. \quad (9)$$

Since a laboratory polarizer kept in  $X$ - $Z$  plane will view  $I_X^{\text{tot}}$  as intensity parallel and  $I_Z^{\text{tot}}$  as intensity perpendicular to incident polarization, the observed fluorescence anisotropy for fluorophores without any intrinsic depolarization will be

$$A' = (I_X^{\text{tot}} - I_Z^{\text{tot}}) / (I_X^{\text{tot}} + 2I_Z^{\text{tot}}). \quad (10)$$

In the above treatment intrinsic causes of depolarization were neglected and the fluorophore was assumed to emit light of same polarization as that of the scattered excitation light. For fluorophore with an intrinsic polarization  $P$  [or anisotropy  $A_0 = 2P / (3 - P)$ ], same analysis leads to the following expression for total detected intensities parallel and perpendicular to incident polarization:

$$\begin{aligned}
 I_X^{\text{obs}} = I_{\parallel}^{\text{obs}} &= (1+P)I_X^{\text{tot}} + (1-P)I_Y^{\text{tot}} + (1-P)I_Z^{\text{tot}}, \\
 I_Y^{\text{obs}} = I_{\perp}^{\text{obs}} &= (1+P)I_Y^{\text{tot}} + (1-P)I_Z^{\text{tot}} + (1-P)I_X^{\text{tot}}, \\
 I_Z^{\text{obs}} = I_{\perp}^{\text{obs}} &= (1+P)I_Z^{\text{tot}} + (1-P)I_Y^{\text{tot}} + (1-P)I_X^{\text{tot}}.
 \end{aligned} \tag{11}$$

The value for anisotropy can then be calculated as

$$A' = (I_X^{\text{obs}} - I_Z^{\text{obs}}) / (I_X^{\text{obs}} + 2I_Z^{\text{obs}}). \tag{12}$$

Single scattering at fluorescence emission depolarizes light in the same manner as that of single scattering at excitation wavelength. Proceeding in a similar way, it can be easily shown that the expression for observed fluorescence anisotropy due to single scattering at fluorescence emission wavelength is identical to Eq. (12).

### B. Depolarization of fluorescence in Rayleigh approximation

The theory developed in the preceding section is valid for spherical scatterers of any size. If the size of the scatterer is very small ( $a \ll \lambda$ ) (Rayleigh region) Mie scattering phase functions [ $P_2(\theta)$  and  $P_1(\theta)$ ] can be replaced by dipole scattering phase functions. The expressions for scattering phase functions polarized parallel and perpendicular to scattering plane can, therefore, be written as [9]

$$P_2(\theta) \approx [9|a_1|^2/4] \cos^2 \theta \quad \text{and} \quad P_1(\theta) \approx [9|a_1|^2/4], \tag{13}$$

where  $a_1 = -(i2x^3/3)\{(m^2-1)/(m^2+2)\}$ .

Here  $x$  is the scatterer size parameter and  $m$  is the complex refractive index. Putting the values of  $P_2(\theta)$  and  $P_1(\theta)$  in Eq. (7) and then using Eq. (9) and (11), we obtain

$$I_X^{\text{obs}} = I_{\parallel}^{\text{obs}} \approx (10+6P)/15. \tag{14}$$

Similarly putting the values of  $P_2(\theta)$  and  $P_1(\theta)$  in Eq. (7) and then using Eq. (9) and (11), we obtain

$$I_Y^{\text{obs}} = I_Z^{\text{obs}} = I_{\perp}^{\text{obs}} \approx (10-8P)/15. \tag{15}$$

The expression for observed anisotropy will thus be

$$A' = 0.7 A_0 \tag{16}$$

where

$$A_0 = 2P/(3-P).$$

This result is identical to that obtained by Teale [2] using dipole scattering approximation.

### C. Multiple scattering consideration

In the previous section, we derived an expression for reduction in fluorescence anisotropy after single scattering at excitation or emission wavelength. In order to work out anisotropy of fluorescence from fluorophores embedded in a scattering medium, the effect of multiple scattering needs to be incorporated. For this, we follow the approach of Wu *et al.* [10,11], who used a photon migration model to obtain

an analytical relationship between the bulk fluorescence from fluorophores embedded in a scattering medium and the intrinsic fluorescence. It was shown that the bulk fluorescence is given by [11]

$$\begin{aligned}
 F(\lambda_x, \lambda_m) &= \sum_{n=1}^{\infty} f_n(g) \left\{ \sum_{m=0}^{n-1} a^m(\lambda_x) [1 - a(\lambda_x)] \right. \\
 &\quad \left. \times \phi(\lambda_x, \lambda_m) a^{n-m-1}(\lambda_m) \right\},
 \end{aligned} \tag{17}$$

where  $a(\lambda_x)$  and  $a(\lambda_m)$ , the scattering albedos at excitation and emission wavelengths, are given by

$$a(\lambda_x) = [\mu_s^x / (\mu_s^x + \mu_a^x)]$$

and

$$a(\lambda_m) = [\mu_s^m / (\mu_s^m + \mu_a^m)],$$

$\mu_s$  and  $\mu_a$  are the scattering and absorption coefficient, superscript  $x$  and  $m$  refers to excitation and emission wavelength, respectively;  $\phi(\lambda_x, \lambda_m)$  is the intrinsic fluorescence from a fluorophore embedded in the scattering medium;  $f_n(g)$  is the probability distribution function that a photon will escape from a semiinfinite scattering medium after  $n$  scattering events,  $g$  being the average cosine of scattering angle, and can be approximated by the following analytical expression [10]:

$$f_n(g) = \{1 - \exp[-0.45(1-g)n]\}^2 \times [3/2\pi(1-g)]^{1/2} n^{-3/2}. \tag{18}$$

To account for the isotropic emission of fluorescence, an effective anisotropy coefficient  $g_{\text{eff}}$  was introduced [11]. It was defined as the average value of  $(N-1)$  forward directed scattering events with anisotropy coefficient  $g$  and a single isotropic fluorescence event, i.e.,  $g_{\text{fluorescence}} = 0$ ,

$$g_{\text{eff}} = (N-1)g/N.$$

The procedure adopted by Wu, Feld, and Rava was followed for choosing  $N$ . Further for simplicity  $g$  was assumed to be constant over the excitation and emission wavelength region. The expression for fluorescence anisotropy from fluorophores embedded in a scattering medium was obtained as

$$\begin{aligned}
 A_{\text{obs}} &= \left\{ A_0 \sum_{n=1}^{\infty} f_n(g) \left\{ \sum_{m=0}^{n-1} a^m(\lambda_x) [1 - a(\lambda_x)] \right. \right. \\
 &\quad \left. \left. \times \phi(\lambda_x, \lambda_m) a^{n-m-1}(\lambda_m) \right\} \right. \\
 &\quad \left. \times r_x^{m+1} r_m^{n-m-1} \right\} / F(\lambda_x, \lambda_m),
 \end{aligned} \tag{19}$$

where  $r_x$  and  $r_m$  are the reduction in anisotropy after single scattering at excitation and emission wavelength, respectively, and  $A_0$  is the intrinsic anisotropy of fluorescence from fluorophores in absence of scattering.

### III. EXPERIMENTAL METHODS

In order to experimentally determine the dependence of the anisotropy of fluorescence on scatterer size and concentration, two types of samples were prepared. All the samples used methylene blue ( $80 \mu\text{M}$ ) (Sigma Chemicals, U.S.A.) as absorber and polystyrene microspheres (diameter 0.3 or  $0.61 \mu\text{m}$ ) (Bangs Lab., U.S.A.) as scatterers. One set used reduced form of NADH ( $80 \mu\text{M}$ ) (Sigma Chemicals, U.S.A.) as fluorophores and the other used riboflavins ( $20 \mu\text{M}$ ) (Sigma Chemicals, U.S.A.) as fluorophores. While preparing microsphere suspension, a small amount (0.1% by weight) of surfactant (sodium dodecyl sulphate) (Sdfine Chemicals, India) was added to the solvent (distilled water) to maintain their monodispersity. The microsphere suspension was contained in a quartz cuvette with a path length of 10 mm. The absorption coefficients ( $\mu_a$ ) of the two solutions, one prepared with  $80\text{-}\mu\text{M}$  NADH and  $80\text{-}\mu\text{M}$  methylene blue, and the other with  $20\text{-}\mu\text{M}$  riboflavins and  $80\text{-}\mu\text{M}$  methylene blue, were measured separately using a spectrophotometer before adding these to the microsphere suspension. While preparing the two types of samples used in the validation studies, the concentration of the fluorophore and absorber was kept constant and the concentration of scatterer was varied. The choice of the concentration of fluorophores and absorber is not critical. The values were chosen to have good fluorescence signal and to ensure that scattering dominates over absorption ( $\mu_s > \mu_n$ ).

A commercial spectrofluorometer (SPEX, Fluorolog II) was used to record polarized fluorescence spectra at excitation wavelengths 340 and 460 nm, respectively, for the samples prepared using NADH and riboflavins as fluorophores. The bandpass for both the excitation and emission monochromator was 1.7 nm. The integration time was kept 0.2 s and the scan step was chosen 1 nm while recording emission spectrum. The excitation light, from a 450-W xenon lamp, was incident on the sample surface with a spot size of  $2 \times 4$  mm. The fluorescence was collected at  $90^\circ$  angle with respect to the excitation light. The excitation polarizer was oriented vertically and the polarized emission spectra were recorded with emission polarizer oriented in horizontal ( $\perp$ ) and vertical ( $\parallel$ ) positions, respectively. All the spectra were corrected for the system response with the correction curve provided with the instrument. The values for fluorescence anisotropy ( $A$ ) at 440 nm emission for the samples with NADH as fluorophores and at 540 nm emission for the samples with Riboflavins as fluorophores were calculated using the following equation [1]:

$$A = [I_{\parallel} - GI_{\perp}] / [I_{\parallel} + 2GI_{\perp}]. \quad (20)$$

Here  $G(I_{HV}/I_{HH})$  is the ratio of the sensitivity of the instrument to the vertical and horizontally polarized light. For measuring spectral dependence of  $G$ , very dilute solution (10 ppm) of glycogen in distilled water was taken in a quartz cuvette and synchronous scan over the wavelength region 300–600 nm was recorded with zero offset between excitation and emission monochromator. The excitation polarizer was kept horizontal and emission polarizer was placed at

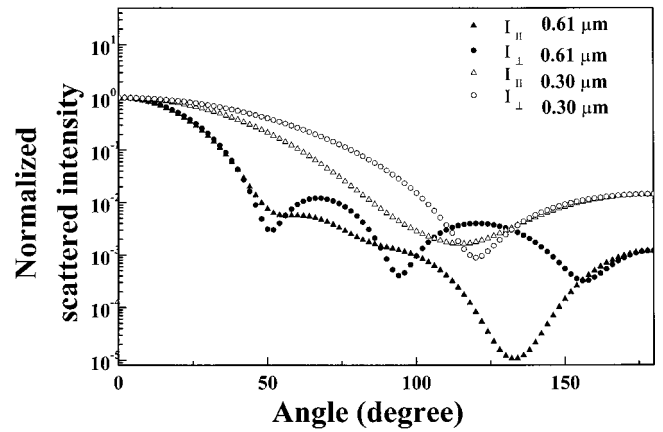


FIG. 2. Scattering phase function computed at 540 nm for the  $0.3\text{-}\mu\text{m}$  (open symbol) and  $0.61\text{-}\mu\text{m}$  diameter (solid symbol) microsphere suspension. The triangles correspond to scattered intensity with field vector parallel to the scattering plane and the circles correspond to scattered intensity with field vector perpendicular to the scattering plane for both scatterers.

horizontal ( $I_{HH}$ ) and vertical ( $I_{HV}$ ) orientations. The details of this measurement are provided in Ref. [12].

### IV. RESULTS AND DISCUSSION

The values for the factor  $r_0$  for scatterers with different size parameter were calculated following the procedure described in Sec. II A. For these calculations the refractive index of the scatterer was taken as 1.59 and that of the surrounding medium 1.33. The scattering phase functions  $P_2(\theta)$  and  $P_1(\theta)$  and the value for average cosine of scattering angle ( $g$ ) were computed using Mie theory for different scatterer size parameters ( $x = 2\pi aN/\lambda$ ) [6]. In Fig. 2, we show the computed phase functions (at  $\lambda = 540$  nm) for scatterers

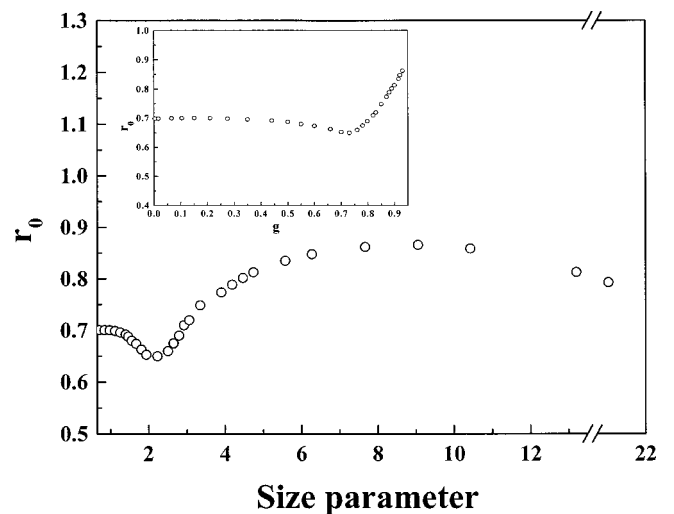


FIG. 3. Variation of the value for the factor  $r_0$  defined as the ratio of fluorescence anisotropy after single scattering to the initial anisotropy ( $A_0$ ) as a function of dimensionless scatterer size parameter. The inset shows variation of  $r_0$  with average cosine of scattering angle ( $g$ ) of the scatterer.



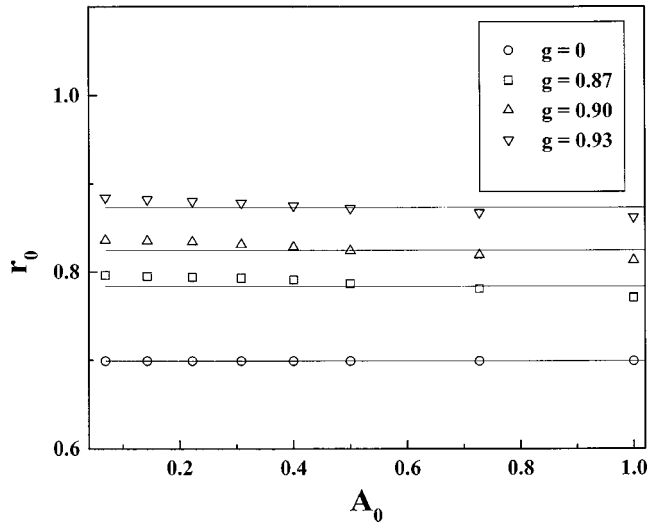


FIG. 4. Variation of the value for  $r_0$  as a function of initial value of anisotropy ( $A_0$ ). The values for average cosine of scattering angle ( $g$ ) are listed in the legend.

with 0.3 and 0.61  $\mu\text{m}$  diameter that were used for our validation studies. The phase functions shown have been normalized with respect to the intensity for forward scattering ( $\theta=0^\circ$ ). In Fig. 3, we show the computed values for the factor  $r_0$  for scatterers with different size parameter ( $x$ ). The inset of the figure shows the dependence of  $r_0$  on average cosine of scattering angle ( $g$ ) calculated for the same scatterers. No intrinsic depolarization was assumed for these calculations. It is evident from the figure that the value for  $r_0$  is independent of scatterer size parameter in the Rayleigh region ( $x < 1$ ). In the intermediate region ( $1 < x < 2.8$ ) the value for  $r_0$  reduces below 0.7. This is due to the presence of characteristic backscattered lobes in the phase function [ $P_2(\theta)$  and  $P_1(\theta)$ ] for this parameter window (Fig. 2). For  $x > 2.8$ , the value for the factor  $r_0$  increases. This is expected because the larger the value for size parameter more predominant is forward scattering and hence lesser should be the depolarization. It is pertinent to note here that for  $x > 9$  the value of  $r_0$  is again observed to decrease. A similar behavior in the characteristic length of depolarization for elastically scattered light was observed by Bicout *et al.* [5] and was attributed to Mie resonances.

The value for the anisotropy of fluorescence after single scattering is also expected to depend on the initial anisotropy value [see Eqs. (11) and (12)]. Computations were therefore performed for different values of initial anisotropy ( $A_0$ ) and the results are shown in Fig. 4. The corresponding values for  $g$  are also listed in the figure. For a given  $g$ , the factor  $r_0$  slightly decreases with increasing value of initial anisotropy ( $A_0$ ). However, the dependence is rather weak. In Rayleigh scattering approximation ( $g \sim 0$ ), the factor  $r_0$  is independent of  $A_0$  and has a value of 0.7 that is consistent with the earlier results of Teale [2].

In order to work out anisotropy of fluorescence from a turbid sample one has to account for multiple scattering. The effect of multiple scattering was incorporated following the treatment of Sec. II C. For these calculations the scattering

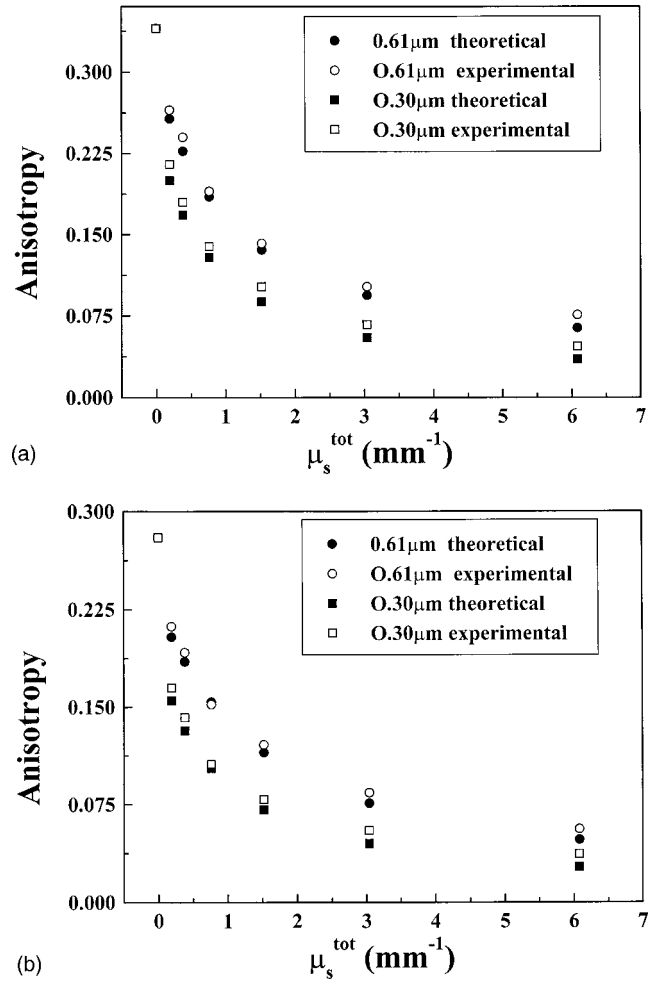


FIG. 5. Experimentally measured values of anisotropy of 340-nm excited 440-nm fluorescence (open symbols) for the scattering samples with NADH as fluorophores as a function of scattering coefficients [ $(\mu_s^{\text{tot}} = (\mu_s^x + \mu_s^m))$ ]. Circles represent samples prepared with 0.61- $\mu\text{m}$  diameter microspheres and squares represent samples prepared with 0.3- $\mu\text{m}$  diameter microspheres. The solid symbols show the theoretically computed values for anisotropy. (b) Experimentally measured values of anisotropy of 460-nm excited 540-nm fluorescence (open symbols) for the scattering samples with riboflavins as fluorophores as a function of scattering coefficients [ $(\mu_s^{\text{tot}} = (\mu_s^x + \mu_s^m))$ ]. Circles represent samples prepared with 0.61- $\mu\text{m}$  diameter microspheres and squares represent samples prepared with 0.3- $\mu\text{m}$  diameter microspheres. The solid symbols show the theoretically computed values for anisotropy.

coefficients ( $\mu_s$ ) at different wavelengths were calculated using the relation

$$\mu_s = N_c A_s Q_s, \quad (21)$$

where  $A_s$  is the area of cross section of the scatterers,  $N_c$  is the concentration of scatterers, and  $Q_s$  is the single scattering efficiency and was computed using Mie's theory [9]. For  $\mu_a$ , the spectrophotometrically measured values were used and the value for  $A_0$  was taken as the value for anisotropy measured in samples without scatterers. For these calculations

the factor  $r_0$  was assumed constant because as discussed earlier (Fig. 4), the value for  $r_0$  does not change significantly with a change in initial anisotropy.

In Fig. 5(a), we show the experimentally measured values of anisotropy of 340-nm excited 440-nm fluorescence for the scattering samples with NADH as fluorophores as a function of scattering coefficients [ $(\mu_s^{\text{tot}} = (\mu_s^x + \mu_s^m))$ ]. In Fig. 5(b), measured fluorescence anisotropy for 460-nm excited 540-nm fluorescence for the scattering samples with riboflavins as fluorophores are shown as a function of scattering coefficient [ $(\mu_s^{\text{tot}} = (\mu_s^x + \mu_s^m))$ ]. Circles represent scattering samples prepared with 0.61- $\mu\text{m}$  diameter microspheres and squares represent samples prepared with 0.3- $\mu\text{m}$  diameter microspheres. The theoretically computed values for anisotropy using Eq. (19) of Sec. II C are shown as solid symbols in both the figures. The agreement between the theoretically computed values and the experimentally measured values is seen to be quite satisfactory for all the samples.

For 0.3- $\mu\text{m}$  diameter microspheres the values for the scatterer size parameter range from 2.08 to 3.3 for the excitation and emission wavelengths used in the experiment. The corresponding values for the 0.61- $\mu\text{m}$  microspheres range from 4.24 to 6.73. Therefore, for our experiment the factor  $r_0$  is always larger for 0.61- $\mu\text{m}$  scatterer than 0.3- $\mu\text{m}$  scatterer.

Hence depolarization of fluorescence will be higher for 0.3- $\mu\text{m}$  diameter microspheres as has been observed experimentally [Figs. 5(a) and (b)]. It may be pertinent to note here that for the scatterer size parameter window  $1 < x < 2.8$ , the value for  $r_0$  can be smaller for larger value of scatterer size parameter. It is therefore possible to have a situation where depolarization is more for larger size scatterer. We are planning experiments with other scatterers of appropriate size to verify this aspect.

## V. CONCLUSIONS

We have shown that the ratio of the anisotropy of fluorescence after one scattering at excitation or emission wavelength to the initial value depends on the size parameter of scatterer. This value was found to vary between 0.65 to 0.85 for a variation in scatterer size parameter of  $0 < x < 20$ . The theory developed can be used to work out anisotropy reduction after successive scattering for fluorophores embedded in any monodisperse scattering medium with known scatterer size and refractive index. Extension to a polydisperse scattering medium with a known distribution of scatterer size is straightforward.

- 
- [1] J. Lackowicz, *Principles of Fluorescence Spectroscopy* (Plenum, New York, 1983).
  - [2] F. W. J. Teale, *Photochem. Photobiol.* **10**, 363 (1969).
  - [3] F. C. Mackintosh, J. X. Zhu, D. J. Pine, and D. A. Weitz, *Phys. Rev. B* **40**, 9342 (1989).
  - [4] J. M. Schmitt, A. H. Gandjbakhche, and R. F. Bonner, *Appl. Opt.* **31**, 6535 (1992).
  - [5] D. Bicout, C. Brosseau, A. S. Martinez, and J. M. Schmitt, *Phys. Rev. E* **49**, 1767 (1994).
  - [6] A. H. Hielscher, J. R. Mourant, and I. J. Bigio, *Appl. Opt.* **36**, 125 (1997).
  - [7] S. P. Morgan, M. P. Khong, and M. G. Somekh, *Appl. Opt.* **36**, 1560 (1997).
  - [8] S. L. Jacques, J. R. Roman, and K. Lee, *Lasers Surg. Med.* **26**, 119 (2000).
  - [9] C. F. Bohren and D. R. Hoffman, *Absorption and Scattering of Light by Small Particles* (Wiley, New York, 1983).
  - [10] J. Wu, F. Patrovi, M. S. Feld, and R. P. Rava, *Appl. Opt.* **32**, 1115 (1993).
  - [11] J. Wu, M. S. Feld, and R. P. Rava, *Appl. Opt.* **32**, 1115 (1993).
  - [12] S. K. Mohanty, N. Ghosh, S. K. Majumder, and P. K. Gupta, *Appl. Opt.* **40**, 1147 (2001).